UC Santa Barbara
UC Santa Barbara Previously Published Works

Title

Telecom-wavelength NV-center analogs in cubic boron nitride

Permalink

https://escholarship.org/uc/item/23h1r0jt

Journal

Physical Review B, 108(4)

ISSN

2469-9950

Authors

Turiansky, Mark E

Van de Walle, Chris G

Publication Date

2023-07-01

DOI

10.1103/physrevb.108.l041102

Copyright Information

Peer reviewed

Telecom-Wavelength NV-Center Analogues in Cubic Boron Nitride

Mark E. Turiansky[1, *] and Chris G. Van de Walle[1, †]

[1]*Materials Department, University of California, Santa Barbara, CA 93106-5050, U.S.A.*

We apply first-principles calculations to investigate V_B-C_B and V_B-Si_B complexes in cubic boron nitride as potential quantum defects. We find that these centers possess a triplet ground-state spin, analogous to that of the prototype quantum defect, the NV center in diamond. In contrast, the main optical transition of these complexes occurs in the telecom O-band, making them appealing for quantum networking applications. Furthermore the coupling to phonons is weaker than in the NV center, resulting in a much larger fraction of photons (22%) being emitted in the zero-phonon line. One inherent drawback of the longer emission wavelength is stronger nonradiative recombination; however, the resulting lower quantum efficiency can be mitigated by cavity coupling.

Quantum defects are point defects or impurities embedded in solids that have properties useful for quantum technologies. The prototype quantum defect is the NV center in diamond, a carbon vacancy neighboring a substitutional N impurity. In the negative charge state, the NV center possesses a triplet ground state, allowing it to act as a spin qubit. The NV center has an optical interface that enables initialization and readout of the ground-state spin.[1] These properties underlie the NV center's ubiquity in quantum-defect research, enabling nanoscale sensing,[2] quantum networking,[3] and long-range entanglement.[4]

Despite these successes, the NV center has various limitations. The optical interface is highly lossy: less than 3% of the emitted photons are in the well-defined quantum state (with a wavelength corresponding to the zero-phonon line) that can be used for entanglement. Furthermore, the emitted photons are in the visible spectrum, which results in considerable losses when transmitted via fiber-optic cables. An alternative to the NV center which emits photons at telecom wavelengths, where fiber-optic losses are minimized,[5] would be highly desirable for networking. Moreover such photons fall into the second near-infrared window, which is advantageous for biological sensing due to reduced interaction with biological tissue.[6]

Cubic boron nitride (c-BN) is a sister compound to diamond, with similar properties such as an ultra-wide band gap, excellent stability, high thermal conductivity,[7] and controllable dopability.[8–10] The hexagonal phase of boron nitride has received much attention as a host for quantum defects,[11,12] but comparatively little attention has been paid to c-BN, likely due to the difficulty in growing high-quality single crystals. Still, steady progress has been made,[13–18] and it is expected that the quality will continue to improve. Photoluminescent centers in c-BN have been observed,[19] but their potential as quantum defects has not been assessed. V_B-O_N in c-BN was proposed as an NV-center analogue,[20,21] but does not offer notable advantages over the NV center. Various defect complexes in c-BN have been calculated,[22] but the calculations relied on semi-local functionals and the ability of those complexes to act as quantum defects was not assessed.

In this Letter, we utilize first-principles calculations based on hybrid density functional theory to demonstrate that neutral V_B-C_B and V_B-Si_B complexes in c-BN are attractive quantum defects. We find that they possess a triplet ground state, similar to the NV center, which enables them to act as spin qubits. We calculate the zero-field splitting and hyperfine parameters to aid in experimental identification. The complexes emit photons at telecom wavelengths within the O-band (1260-1360 nm), making them useful for applications in long-range quantum networking. Moreover the coupling to phonons is drastically smaller than in the NV center: we find that 22% of the emitted photons are in the zero-phonon line and therefore in a well-defined quantum state. Lastly, we quantitatively evaluate the radiative and nonradiative transition rates.

For our calculations, we use hybrid density functional theory within the projector augmented-wave formalism[23] as implemented in the VASP code.[24] We retain Fourier components in the plane-wave basis up to an energy of 520 eV. We use the hybrid functional of Heyd, Scuseria, and Ernzerhof[25] with the fraction of Hartree-Fock exchange set to 33%. These parameters result in an equilibrium lattice parameter $a = 3.59$ Å and an indirect band gap of 6.26 eV, in agreement with the experimental values of 3.62 Å[26] and 6.36 eV.[27]

We investigate defects in a 216-atom supercell obtained from a $3 \times 3 \times 3$ multiple of the 8-atom conventional unit cell. Lattice parameters of the supercell are held fixed; the atomic coordinates are relaxed until forces are below 10 meV/Å. The Brillouin zone is integrated with a single special point (1/4, 1/4, 1/4).[28] Spin polarization is explicitly taken into account.

The formation energy E^f of a given defect X^q in charge state q is defined as[29]

$$E^f[X^q] = E_\text{tot}[X^q] - E_\text{tot}[c\text{-BN}] - \sum_i n_i \mu_i + q E_\text{F} + \Delta^q .$$

(1)

E_tot is the total energy extracted from a supercell calculation, and E_F is the Fermi level. n_i is the number of atoms of atomic species i added to ($n_i > 0$) or removed from ($n_i < 0$) the supercell, and μ_i is the corre-

sponding chemical potential. $\mu_i = E_i + \Delta\mu_i$, where E_i is the single-atom energy for the reference phase (e.g., bulk B for μ_B). Under N-rich growth conditions, $\Delta\mu_N = 0$ and $\Delta\mu_B = -2.79$ eV, which is the calculated formation enthalpy of c-BN. For the incorporation of impurities, we consider the secondary phases $B_{13}C_2$ with enthalpy -0.82 eV and Si_3N_4 with enthalpy -9.12 eV. Finite-size effects resulting from simulating a charged system in periodic boundary conditions are accounted for in the correction term Δ^q.[30]

The formation energies of the investigated defects are shown in Fig. 1 for N-rich conditions, which represent the most favorable conditions for incorporation of both V_B and impurities on the B site. Boron vacancies act as acceptors while C_B and Si_B act as donors: these species will therefore be attracted by a Coulomb interaction. We will focus on the neutral charge state of V_B-C_B and V_B-Si_B, since this corresponds to the desired triplet state. Considering $(V_B$-$C_B)^0$ as formed from binding V_B^- to C_B^+, we calculate a binding energy of 1.33 eV. It is also possible that V_B-C_B is first formed in a $-$ or $2-$ charge state: if we consider the binding of C_B^+ to the appropriate charge state of V_B to maintain charge neutrality we find a binding energy of 1.97 eV for $(V_B$-$C_B)^-$ and 2.56 eV for $(V_B$-$C_B)^{2-}$. The similarly calculated binding energy is 1.47 eV for $(V_B$-$Si_B)^0$, 2.25 eV for $(V_B$-$Si_B)^-$, and 2.89 eV for $(V_B$-$Si_B)^{2-}$. These sizeable binding energies ensure that, once formed, the complexes will remain stable.
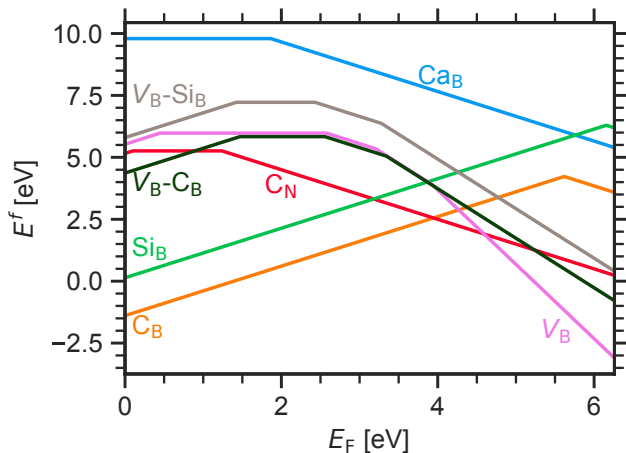

FIG. 1. Formation energies E^f of the substitutional impurities (C_B, C_N, Si_B, and Ca_B), V_B, and impurity-vacancy complexes (V_B-C_B and V_B-Si_B) as a function of the Fermi level E_F.

The desired triplet ground state, which allows these centers to act as spin qubits, is achieved for the neutral charge state of V_B-C_B and V_B-Si_B. c-BN is a high-symmetry crystal with point group T_d. In the absence of atomic relaxation, the introduction of a vacancy and impurity on a second-nearest-neighbor site reduces the symmetry to C_{1h}. In our calculations, we find a slight distortion that lowers the symmetry of the complex to C_1. The distortion is more severe in the case of Si, likely due to the larger size of the impurity.

The Kohn-Sham states of the complexes in the spin-minority channel are shown in Fig. 2. In the spin-majority channel, all defect orbitals are occupied and slightly above or resonant with the valence band. We explicitly verified that the triplet state is the ground state by also calculating the singlet state. Our calculations predict that the lowest singlet state is 140 meV above the triplet ground state of V_B-C_B and 72 meV above the triplet ground state of V_B-Si_B. It is worth noting that the singlet states exhibit "antiferromagnetism", which is indicative of "broken-symmetry" character.[31,32] Various studies have shown that the broken-symmetry states provide a reliable description of energy differences within DFT.[31,32]

Part of the appeal of the NV center is the ability to optically initialize, control, and readout the ground-state spin.[1] These dynamics are a result of an intersystem crossing from the triplet manifold to the singlet manifold and subsequent relaxation. A full assessment of the spin-dependent transition rates and the higher-lying singlet excited states is beyond the scope of this manuscript. It is worthwhile to note that even in the absence of an efficient intersystem crossing, all optical techniques exist to manipulate the spin.[33]
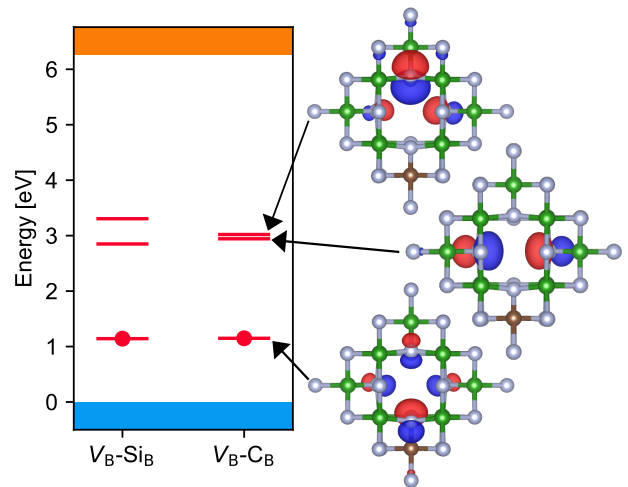

FIG. 2. Schematic position of the Kohn-Sham states in the spin-minority channel with respect to the band edges. Occupied levels are depicted with a red circle. The valence band is shown in blue, and the conduction band in orange. The charge density isosurfaces for the Kohn-Sham states of V_B-C_B are shown on the right. B atoms are shown in green, N in grey, and C in brown. The isosurfaces are colored by the phase of the wavefunction, with red and blue indicating opposite signs.

Due to the low symmetry of the center, all three magnetic sublevels are non-degenerate at zero field. In Table I we list our computed zero-field splittings arising from spin-spin dipolar interactions; these splittings are essential properties for microwave control and also aid in

experimental identification. We also computed the hyperfine coupling to the nearest-neighbor ^{14}N nuclei (Table I). We find that there is negligible spin density (A values less than 3 MHz) on the nearest-neighbor N nucleus closest to the impurity; the reported values are for the other three nuclei. For V_B-C_B, the values for these three N neighbors are the same to within 1 MHz. For V_B-Si_B, which has lower symmetry and hence a more asymmetric spin density, we provide values for the individual N atoms.

TABLE I. The calculated zero-field splitting (D_x, D_y, D_z) and hyperfine (A_{xx}, A_{yy}, A_{zz}) parameters after diagonalization.

		V_B-C_B	V_B-Si_B
Zero-field Splitting [MHz]	D_x	-1490	-3030
	D_y	-1280	180
	D_z	2770	2850
^{14}N Hyperfine [MHz]	A_{xx}	30	30/29/21
	A_{yy}	30	30/29/21
	A_{zz}	75	88/79/45

We now consider an optical process in which an electron transitions between the highest occupied level and lowest unoccupied level in the spin minority channel (Fig. 2). To investigate the excited state, we use the constrained occupation ΔSCF approach[34] and construct a configuration coordinate diagram (CCD) using the Nonrad code.[35] The CCD provides a succinct way to rationalize electron-phonon coupling in the context of radiative or nonradiative transitions. The CCDs for V_B-C_B and V_B-Si_B are shown in Fig. 3. Photons produced from the zero-phonon line are in a well-defined quantum state useful for entanglement. We find that the zero-phonon line for V_B-C_B is 0.95 eV or 1305 nm. For V_B-Si_B, the zero-phonon line is 0.89 eV or 1393 nm. Both of these transitions fall within O-band telecom wavelengths, which is excellent for long-range transmission of photons.[5]

Electron-phonon coupling reduces the number of photons emitted into the zero-phonon line and gives rise to a phonon sideband. We can quantify the strength of electron-phonon coupling through the Huang-Rhys factor:[36]

$$S = \frac{1}{2\hbar}(\Delta Q)^2 \Omega_g \, , \quad (2)$$

where Ω_g is the vibrational frequency of the ground state. ΔQ is the mass-weighted difference in atomic geometries and is given by

$$(\Delta Q)^2 = \sum_I M_I |\mathbf{R}_{I,g} - \mathbf{R}_{I,e}|^2 \, , \quad (3)$$

where I labels the atomic sites, M_I is the Ith atomic mass, and $\mathbf{R}_{I,g/e}$ are the coordinates of the Ith site in the ground (g) or excited (e) state. We find a Huang-Rhys factor of $S = 1.51$ for both V_B-C_B and V_B-Si_B. As a result, $\exp(-S) \approx 22\%$ of the photons will be in the

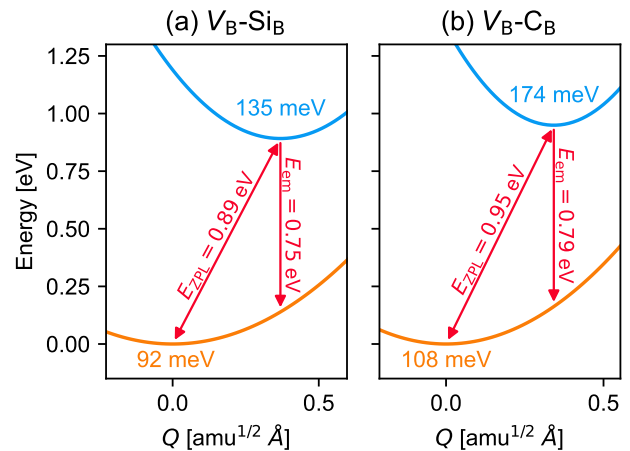FIG. 3. Configuration coordinate diagrams for the spin-conserving optical transition in (a) V_B-Si_B and (b) V_B-C_B. Solid blue lines indicate the potential energy surface of the excited state, and solid orange lines indicate the ground state. Red arrows denote the zero-phonon line energy E_ZPL and the average emission energy E_em. The phonon frequencies for each potential energy surface are labeled.

zero-phonon line. This constitutes almost an order of magnitude improvement over the NV center.

We now address how fast these photons can be produced, by (approximately) calculating the total radiative emission rate using[37]

$$\Gamma_\text{R} = \frac{n_r E_\text{ZPL}^3 \mu^2}{3\pi \epsilon_0 c^3 \hbar^4} \, . \quad (4)$$

Here E_ZPL is the zero-phonon line energy, μ is the transition dipole moment, and n_r is the index of refraction, which takes a value of ≈ 2.1 in c-BN.[38] We find a value of $\Gamma_\text{R} = 5.6$ MHz (7.3 MHz) for V_B-C_B (V_B-Si_B). This value is smaller than that of the NV center,[1] mostly due to the smaller transition energy; however, this is a worthy price to pay for a telecom-wavelength transition.

The quantum efficiency η of the transition is given by

$$\eta = \frac{\Gamma_\text{R}}{\Gamma_\text{R} + \Gamma_\text{NR}} \, , \quad (5)$$

where Γ_NR is the nonradiative transition rate. The nonradiative transition rate enabled by multiphonon emission[37,39] is given by

$$\Gamma_\text{NR} = \frac{2\pi}{\hbar} W_{eg}^2 \sum_m w_m \sum_n |\langle \chi_{em} | \hat{Q} - Q_0 | \chi_{gn} \rangle|^2 \\ \times \delta(E_\text{ZPL} + m\hbar\Omega_e - n\hbar\Omega_g) \, , \quad (6)$$

where w_m is the thermal occupation factor for the mth vibrational mode of the initial state. $\Omega_{e/g}$ are the phonon frequencies of the excited (e) and ground (g) state derived from the configuration coordinate diagram, and Q_0 is the geometry for the perturbative expansion. W_{eg} is the

electron-phonon coupling matrix element. We evaluate the nonradiative transition rate enabled by multiphonon emission[37,39] using the Nonrad code.[35]

We find a nonradiative transition rate of $\Gamma_{NR} =$ 10 GHz (23 GHz) for V_B-C_B (V_B-Si_B) at 4 K. The resulting quantum efficiencies are then 0.05% for V_B-C_B and 0.03% for V_B-Si_B. The low quantum efficiency is not ideal but is not prohibitive. In applications where the ground-state spin is utilized as the qubit, the optical interface simply provides a means of addressing the qubit. For such applications, the quantum efficiency is not a major limitation. However, when the photon itself is used as a qubit or as a means of entanglement, single photons need to be produced on demand:[40] one excitation should result in one photon, which requires 100% quantum efficiency. Fortunately, the low quantum efficiency can be overcome by coupling to a photonic cavity: this increases the photon density of states, significantly enhancing the radiative transition rate and therefore the quantum efficiency.[41]

Photons at telecom wavelengths can also be produced using rare-earth impurities.[42] However, the relevant transitions are electric-dipole forbidden, and thus the corresponding rates are remarkably low (kHz or lower); cavity coupling is necessary to observe the emission in the first place.[40] In that sense, V_B-C_B and V_B-Si_B are an improvement, since they produce photons at a rate several of orders of magnitude faster.

We now return to the issue of achieving the desired triplet state, which corresponds to the neutral charge state and thus requires the Fermi level to be between 1.47 and 2.56 eV for V_B-C_B (1.42–2.43 eV for V_B-Si_B) (Fig. 1). The important role played by the Fermi-level position in achieving the desired spin state of a quantum defect is often overlooked, possibly because it is not appreciated that in the case of the prototype NV center in diamond one benefits from a fortuitous coincidence: N impurities (which are abundantly present when NV is formed) confine the Fermi level to a range where the desired negative charge state of NV is stable.[43] We are not so lucky in the case of the V_B-C_B and V_B-Si_B complexes in c-BN. Both Si_B and C_B act as donors and will thus drive the Fermi level towards the conduction band. V_B acts as a compensating acceptor; when it forms during growth charge neutrality would pin the Fermi level near the intersection point of the formation energies of Si_B (C_B) and V_B (Fig. 1), which is still well outside the range where $(V_B$-$Si_B)^0$ and $(V_B$-$C_B)^0$ are stable. Alternatively, one could first attempt to obtain (largely) uncompensated material doped with Si_B or C_B by suppressing the formation of V_B,[9] and subsequently introduce vacancies with irradiation (as is the common practice for creating the NV center in diamond). However, this is still unlikely to result in neutral complexes.

We therefore need a strategy to control the Fermi level. One possibility is to introduce a dopant that will pin the Fermi level (much like N controls the Fermi level in the case of the NV center in diamond). In the case of the quantum defects in c-BN, we would need to dope with impurities that have either a $(+/0)$ or $(0/-)$ level within the desired Fermi-level range; when such dopants dominate in the charge-neutrality condition they will pin the Fermi level. Our search for such impurities revealed only Ca_B as a suitable candidate (Fig. 1). Unfortunately, Ca_B has an extremely high formation energy. Still, it would be interesting to examine whether any Ca is incorporated in bulk c-BN grown from Ca-containing precursors.[13,14]

Another possibility is to take advantage of carbon itself: when C is incorporated on the N (rather than the B) site, it acts as a deep acceptor. If growth conditions are tuned to favor incorporation of C_N as the dominant impurity, its neutral charge state (assuming a background of donor-type impurities) will pin the Fermi level around 1.24 eV, just shy of the range where $(V_B$-$C_B)^0$ is stable (Fig. 1). Some fraction of C would still incorporate on the B site and would form the V_B-C_B complexes, along with vacancies created by irradiation. While the Fermi level pinned by C_N is slightly outside the range where $(V_B$-$C_B)^0$ is stable, it might actually be brought within that range due to band bending. Since C_N pins the Fermi level low in the gap, some amount of downward bend bending is expected near the surface. Preferential activation of centers in the near-surface region is actually beneficial for optical control and for sensing applications.

Finally we note that the correct charge state can also be achieved if the setup allows applying a gate voltage. In the case of C_N doping, a small positive voltage (referenced to the flat-band position) would lead to downward band bending and bring the Fermi level within the region of stability of $(V_B$-$C_B)^0$ for a range of depths below the surface. This method of control could also conceivably be used to achieve the neutral charge state even in the case where V_B-C_B or V_B-Si_B complexes are formed in other charge states under near-equilibrium conditions, but the Fermi level needs to be moved closer to the valence band.

In conclusion, we have assessed the potential of V_B-C_B and V_B-Si_B in c-BN to act as quantum defects. These complexes possess a triplet ground-state spin, similar to that of the NV center. We evaluated the zero-field splitting and hyperfine parameters, and found that the main optical transition occurs at O-band telecom wavelengths, rendering it suitable for quantum networking applications. Electron-phonon coupling is weaker than in the NV center, resulting in a much larger fraction (22%) of photons to be emitted in the zero-phonon line. While these features are a desirable improvement over the NV center, one drawback of these complexes is their low quantum efficiency. The low energy of the transition is conducive to strong nonradiative recombination enabled by multiphonon emission. Cavity coupling can overcome this low quantum efficiency. Our work on these defect complexes expands the database of potential quantum defects, but also highlights the inherent trade-offs that may be necessary in choosing a quantum defect for various applications.

DATA AVAILABILITY

The data that supports the findings of this study are available from the corresponding author upon reasonable request.

* mturiansky@physics.ucsb.edu

† vandewalle@mrl.ucsb.edu

[1] Á. Gali, Nanophotonics 8, 1907 (2019).

[2] A. Jenkins, M. Pelliccione, G. Yu, X. Ma, X. Li, K. L. Wang, and A. C. B. Jayich, Phys. Rev. Mater. 3, 083801 (2019).

[3] M. Pompili, S. L. N. Hermans, S. Baier, H. K. C. Beukers, P. C. Humphreys, R. N. Schouten, R. F. L. Vermeulen, M. J. Tiggelman, L. dos Santos Martins, B. Dirkse, S. Wehner, and R. Hanson, Science 372, 259 (2021).

[4] H. Bernien, B. Hensen, W. Pfaff, G. Koolstra, M. S. Blok, L. Robledo, T. H. Taminiau, M. Markham, D. J. Twitchen, L. Childress, and R. Hanson, Nature 497, 86 (2013).

[5] G. P. Agrawal, Fiber-Optic Communication Systems, 4th ed., Wiley Series in Microwave and Optical Engineering No. 222 (Wiley, New York, 2010).

[6] Kenry, Y. Duan, and B. Liu, Adv. Mater. 30, 1802394 (2018).

[7] J. Y. Tsao, S. Chowdhury, M. A. Hollis, D. Jena, N. M. Johnson, K. A. Jones, R. J. Kaplar, S. Rajan, C. G. Van de Walle, E. Bellotti, C. L. Chua, R. Collazo, M. E. Coltrin, J. A. Cooper, K. R. Evans, S. Graham, T. A. Grotjohn, E. R. Heller, M. Higashiwaki, M. S. Islam, P. W. Juodawlkis, M. A. Khan, A. D. Koehler, J. H. Leach, U. K. Mishra, R. J. Nemanich, R. C. N. Pilawa-Podgurski, J. B. Shealy, Z. Sitar, M. J. Tadjer, A. F. Witulski, M. Wraback, and J. A. Simmons, Adv. Electron. Mater. 4, 1600501 (2018).

[8] X. W. Zhang, Thin Solid Films 544, 2 (2013).

[9] M. E. Turiansky, D. Wickramaratne, J. L. Lyons, and C. G. Van de Walle, Appl. Phys. Lett. 119, 162105 (2021).

[10] L. Weston, D. Wickramaratne, and C. G. Van de Walle, Phys. Rev. B 96, 100102(R) (2017).

[11] T. T. Tran, C. Elbadawi, D. Totonjian, C. J. Lobo, G. Grosso, H. Moon, D. R. Englund, M. J. Ford, I. Aharonovich, and M. Toth, ACS Nano 10, 7331 (2016).

[12] M. E. Turiansky, A. Alkauskas, L. C. Bassett, and C. G. Van de Walle, Phys. Rev. Lett. 123, 127401 (2019).

[13] S. Nakano, H. Ikawa, and O. Fukunaga, Diam. Relat. Mater. 3, 75 (1994).

[14] O. Fukunaga, S. Nakano, and T. Taniguchi, Diam. Relat. Mater. 13, 1709 (2004).

[15] T. Taniguchi and K. Watanabe, J. Crys. Growth 303, 525 (2007).

[16] Y. Kubota, K. Watanabe, and T. Taniguchi, Jpn. J. Appl. Phys. 46, 311 (2007).

[17] K. Hirama, Y. Taniyasu, S.-i. Karimoto, Y. Krockenberger, and H. Yamamoto, Appl. Phys. Lett. 104, 092113 (2014).

[18] P. Milas, S. Mathab, J. B. Sam Abraham, J. Alam, M. V. S. Chandrashekar, A. J. Robinson, P. M. Vora, B. Ozturk, and M. G. Spencer, AIP Adv. 12, 095303 (2022).

[19] A. Tararan, S. di Sabatino, M. Gatti, T. Taniguchi, K. Watanabe, L. Reining, L. H. G. Tizei, M. Kociak, and A. Zobelli, Phys. Rev. B 98, 094106 (2018).

[20] T. A. Abtew, W. Gao, X. Gao, Y. Y. Sun, S. B. Zhang, and P. Zhang, Phys. Rev. Lett. 113, 136401 (2014).

[21] G. Bian, H. Yuan, N. Zhang, L. Xu, J. Zhang, P. Fan, H. Wang, C. Zhang, G. Shan, Q. Zhang, and J. Fang, Appl. Phys. Lett. 114, 102105 (2019).

[22] W. Orellana and H. Chacham, Phys. Rev. B 62, 10135 (2000); Phys. Rev. B 63, 125205 (2001).

[23] P. E. Blöchl, Phys. Rev. B 50, 17953 (1994).

[24] G. Kresse and J. Furthmüller, Phys. Rev. B 54, 11169 (1996).

[25] J. Heyd, G. E. Scuseria, and M. Ernzerhof, J. Chem. Phys. 118, 8207 (2003); J. Chem. Phys. 124, 219906 (2006).

[26] T. Sōma, A. Sawaoka, and S. Saito, Mater. Res. Bull. 9, 755 (1974).

[27] D. A. Evans, A. G. McGlynn, B. M. Towlson, M. Gunn, D. Jones, T. E. Jenkins, R. Winter, and N. R. J. Poolton, J. Phys.: Condens. Matter 20, 075233 (2008).

[28] A. Baldereschi, Phys. Rev. B 7, 5212 (1973).

[29] C. Freysoldt, B. Grabowski, T. Hickel, J. Neugebauer, G. Kresse, A. Janotti, and C. G. Van de Walle, Rev. Mod. Phys. 86, 253 (2014).

[30] C. Freysoldt, J. Neugebauer, and C. G. Van de Walle, Phys. Rev. Lett. 102, 016402 (2009); Phys. Status Solidi B 248, 1067 (2011).

[31] G. Thiering and A. Gali, Phys. Rev. B 92, 165203 (2015).

[32] J. Gräfenstein, E. Kraka, M. Filatov, and D. Cremer, Int. J. Mol. Sci. 3, 360 (2002).

[33] C. Santori, D. Fattal, S. M. Spillane, M. Fiorentino, R. G. Beausoleil, A. D. Greentree, P. Olivero, M. Draganski, J. R. Rabeau, P. Reichart, B. C. Gibson, S. Rubanov, D. N. Jamieson, and S. Prawer, Opt. Express 14, 7986 (2006).

[34] R. O. Jones and O. Gunnarsson, Rev. Mod. Phys. 61, 689 (1989).

[35] M. E. Turiansky, A. Alkauskas, M. Engel, G. Kresse, D. Wickramaratne, J.-X. Shen, C. E. Dreyer, and C. G. Van de Walle, Comput. Phys. Commun. **267**, 108056 (2021).

[36] A. Alkauskas, J. L. Lyons, D. Steiauf, and C. G. Van de Walle, Phys. Rev. Lett. **109**, 267401 (2012).

[37] A. M. Stoneham, *Theory of Defects in Solids: Electronic Structure of Defects in Insulators and Semiconductors*, Monographs on the Physics and Chemistry of Materials (Clarendon Press, Oxford, 1975).

[38] P. J. Gielisse, S. S. Mitra, J. N. Plendl, R. D. Griffis, L. C. Mansur, R. Marshall, and E. A. Pascoe, Phys. Rev. **155**, 1039 (1967).

[39] A. Alkauskas, Q. Yan, and C. G. Van de Walle, Phys. Rev. B **90**, 075202 (2014).

[40] I. Aharonovich, D. Englund, and M. Toth, Nat. Photonics **10**, 631 (2016).

[41] L. Novotny and B. Hecht, *Principles of Nano-Optics*, 2nd ed. (Cambridge University Press, Cambridge, 2012).

[42] P. Stevenson, C. M. Phenicie, I. Gray, S. P. Horvath, S. Welinski, A. M. Ferrenti, A. Ferrier, P. Goldner, S. Das, R. Ramesh, R. J. Cava, N. P. de Leon, and J. D. Thompson, Phys. Rev. B **105**, 224106 (2022).

[43] J. R. Weber, W. F. Koehl, J. B. Varley, A. Janotti, and B. B. Buckley, Proc. Natl. Acad. Sci. U.S.A. **107**, 8513 (2010).